

A Magnetic $\alpha\omega$ Dynamo in Active Galactic Nuclei Disks: I. The Hydrodynamics of Star-Disk Collisions and Keplerian Flow

Vladimir I. Pariev^{1,2} and Stirling A. Colgate

Theoretical Astrophysics Group, T-6, Los Alamos National Laboratory, Los Alamos, NM 87545

ABSTRACT

A magnetic field dynamo in the inner regions of the accretion disk surrounding the supermassive black holes in Active Galactic Nuclei (AGNs) may be the mechanism for the generation of magnetic fields in galaxies and in extragalactic space. We argue that the two coherent motions produced by 1) the Keplerian motion and 2) star-disk collisions, numerous in the inner region of AGN accretion disks, are both basic to the formation of a robust, coherent dynamo and consequently the generation of large scale magnetic fields. In addition we find that the predicted rate, 10 to 100 per year at $\sim 1000r_g$, r_g the gravitational radius, and the consequences of star-disk collisions are qualitatively, at least, not inconsistent with observations of broad emission and absorption lines. They are frequent enough to account for an integrated dynamo gain, e^{10^9} at $100r_g$, many orders of magnitude greater than required to amplify any seed field no matter how small. The existence of extra-galactic, coherent, large scale magnetic fields whose energies greatly exceed all but massive black hole energies is recognized. In paper II (Pariev, Colgate & Finn 2006) we argue that in order to produce a dynamo that can access the free energy of black hole formation and produce all the magnetic flux in a coherent fashion the existence of these two coherent motions in a conducting fluid is required. The differential winding of Keplerian motion is obvious, but the disk structure depends upon the model of " α ", the transport coefficient of angular momentum chosen. The counter rotation of driven plumes in a rotating frame is less well known, but fortunately the magnetic effect is independent of the disk model. Both motions are discussed in this paper, paper I. The description of the two motions are preliminary to two theoretical derivations and one numerical simulation of the $\alpha\omega$ dynamo in paper II.

Subject headings: accretion, accretion disks — magnetic fields — galaxies: active

1. Introduction

The need for a magnetic dynamo to produce and amplify the immense magnetic fields observed external to galaxies and in clusters of galaxies has long been recognized. The theory of kinematic

¹Lebedev Physical Institute, Leninsky Prospect 53, Moscow 119991, Russia

²Currently at Physics Department, University of Wisconsin-Madison, 1150 University Ave., Madison, WI 53706

magnetic dynamos has had a long history and is a well developed subject by now. There are numerous monographs and review articles devoted to the magnetic dynamos in astrophysics, some of which are: Parker (1979); Moffatt (1978); Stix (1975); Cowling (1981); Roberts & Soward (1992); Childress et al. (1990); Zeldovich, Ruzmaikin, & Sokoloff (1983); Priest (1982); Busse (1991); Krause & Rädler (1980); Biskamp (1993); Mestel (1999). Hundreds of papers on magnetic dynamos are published each year. Three main astrophysical areas, in which dynamos are involved, are the generation of magnetic fields in the convective zones of planets and stars, in differentially rotating spiral galaxies, and in the accretion disks around compact objects. The possibility of production of magnetic fields in the central parts of the black hole accretion disks in AGN has been pointed out by Chakrabarti, Rosner, & Vainshtein (1994) and the need and possibility for a robust dynamo by Colgate & Li (1997). Dynamos have been also observed in the laboratory in the Riga experiment (Gailitis et al. 2000, 2001) and in Karlsruhe experiment (Stieglitz & Müller 2001). Recently, counter rotating, opposed jets or open-flow geometries, such as the the Von Kármán Sodium (VKS) Experiment and the Madison Dynamo Experiment, have been designed to explore less constrained flows (Bourgoin et al. 2004; Spence et al. 2006). So far, neither of these experiments have reported sustained magnetic field generation despite predictions of positive gain in laminar flow theory and calculations. The null result has been ascribed to the deleterious effects of enhanced turbulent diffusion of large-scale turbulence.

1.1. The Need for a Robust Astrophysical Dynamo

Why, with all the thousands of research papers, very many successes, and even experimental verification of dynamo theory in constrained flows is there a need for a new paradigm for the generation of intergalactic scale astrophysical magnetic fields? We claim that the plume-driven $\alpha\omega$ dynamo in the black hole accretion disk is a unique solution to the need for the largest dynamos of the universe, because the flow is naturally constrained by a gradient in angular momentum and by the transient dynamical behavior of plumes in contrast to the large turbulence of unconstrained flows. (A discussion of the role of convective plume-driven $\alpha\omega$ dynamos in stars will be reserved for another paper, because the mechanism of the production of large scale plumes in the convective zone of stars is radically different from the production of plumes by high velocity stars plunging frequently through the accretion disk.)

The minimum energy inferred from radio emission observations of structures or so-called radio lobes within clusters and external to clusters by both synchrotron emission and Faraday rotation (Kronberg 1994; Kronberg et al. 2001) are so large, $\sim 10^{59}$ ergs and up to $\sim 10^{61}$ ergs respectively, compared to galactic energies in fields 10^{-7} as large and gravitational binding energies 10^{-3} as large, that only the energy of formation of the central massive black hole (hereafter, CMBH) of every galaxy in its AGN phase, $\sim 10^{62}$ ergs, becomes the most feasible astrophysical known source of so much energy. This statement is based upon the recognition that $\sim 10^8$ neutron stars have been created in the galaxy in a Hubble time, or only $\sim 10^6$ in the life time of a radio lobe of

$\sim 10^8$ yr. Each supernova results in 10^{51} ergs of kinetic energy, the rest being emitted in neutrinos so that $\sim 10^{57}$ ergs of kinetic energy becomes available for the production of magnetic energy within the necessary time. If one considers the difficulty of summing the magnetic field from many, presumably incoherent sources, the likelihood of many stellar sources contributing to the coherent field of radio lobes seems remote.

In order to access this energy of formation the conversion of kinetic to magnetic energy is required. This in turn requires a mechanism to multiply or exponentiate an initial field up to the back reaction limit. This limit is where the Ampere force does a large work to significantly alter the accretion motion thus converting the kinetic energy to magnetic energy. Because the specific angular momentum of matter accreted onto the CMBH is $\sim 10^3$ to 10^4 greater than possible for accretion at r_g , the result is the universal Keplerian motion of an accretion disk and so the access of this free energy must be in the form of a back reaction torque that transforms kinetic to magnetic energy.

A robust dynamo is one that can potentially convert a large fraction of the available mechanical energy or free energy of the accretion disk into magnetic energy. A further advantage of the $\alpha\omega$ dynamo in the CMBH accretion disk is that the exponential gain within 100 gravitational radii of the CMBH is so large, some fraction f per turn, or gain $= e^{fN}$, $N \sim 10^9$ turns in the 10^8 years of formation, that the origin and strength of the initial (seed) field becomes moot.

1.2. The Robust $\alpha\omega$ Dynamo

Such a dynamo has conceptually become feasible because of the recognition of a relatively new, coherent, large scale, robust source of helicity. Helicity generation, in the sense of the $\alpha\omega$ dynamo, is the driven deformation of the conducting fluid that converts an amplified (by differential winding) toroidal field back into the initial, (radial), poloidal field. In our case it is caused by the rotation of driven, diverging plumes in a rotating frame (Beckley et al. 2003; Mestel 1999; Colgate & Li 1999). The advantage of driven plumes as a source of helicity as compared to turbulent motions within the disk is that the flow displaces fluid and entrapped flux well above the disk, several scale heights, and then rotates the flux on average a quarter turn before merging again into the disk. Such an ideal deformation is then a large coherent (single direction) source of helicity. These plumes are presumably driven by many stars in orbits repeatedly plunging through the disk, but comprising only a small mass fraction, $\sim 10^{-3}$, of the matter accreted to form and grow the CMBH to $\sim 10^8 M_\odot$. The twisting or relative rotation of the plumes occurs because of partially conserved angular momentum of the plume itself as its moment of inertia increases due to its expansion or divergence while progressing in height. The repeatable fractional turn before merging with the disk occurs because the cooling plume matter falls back to the disk in half a turn of the disk. This translation and rotation twists the embedded toroidal magnetic field. Furthermore, the angle of twist is in the same direction for all plumes, opposite to the rotation of the disk, and furthermore the angle of this twist is limited to $\Delta\phi \simeq -\pi/2$ radians of rotation for each occurrence. This

nearly ideal repetitive driven deformation leads to a robust dynamo, one where both motions are not likely to be easily damped by back reaction except at the full Keplerian stress. Such a dynamo is not dependent upon a net helicity derived from random turbulent motions. The limitation of turbulently derived helicity due to early back reaction is discussed later, but first we discuss the preference for a finite angle, specifically $(2n + 1)\pi/4$ angle of rotation in n periods of rotation for an effective helicity. (Preferably $n = 0$.)

1.3. The Original $\alpha\omega$ Dynamo

The original proposal of Parker (1955, 1979) of the $\alpha\omega$ dynamo in rotationally sheared conducting flows, seemed to be the logical answer to the problem of creating the large, highly organized fields of stars and galaxies as revealed by polarized synchrotron emission and Faraday rotation maps. Here the radial component of a poloidal field is wrapped up by differential rotation into a much stronger toroidal field. Then as proposed by Parker, cyclonic motions of geostrophic flow twist and displace axially a fraction of the toroidal flux back into the poloidal direction. Subsequent merger of this small component of poloidal flux with the large scale original poloidal flux by resistive diffusion or reconnection completed the cycle. The later process of merging the small scales to create the large scales is referred to as mean field dynamo theory. There were two apparently insurmountable problems with this theory. The first, as argued by Moffatt (1978) and as discussed in Roberts & Soward (1992) was that geostrophic cyclonic flows, with negative pressure on axis, make very many revolutions before dissipating therefore reconnecting the flux in an arbitrary orientation. Hence, the orientation of any newly formed component of poloidal flux would be averaged to near zero. The star-disk driven plumes, on the other hand, avoid this difficulty by falling back to the disk in less than π revolutions of rotation, thereby terminating further rotation by fluid merging within the disk. The second difficulty was that the large dimensions of interstellar space and finite resistivity ensured a near infinite magnetic Reynolds number, $Rm = Lv/\eta$ (L the dimension, v the velocity and η the resistivity), so that, in general, the resistive reconnection time would become large compared to the age of the astrophysical object. Consequently newly minted poloidal flux would never merge with the original poloidal flux.

Currently, although the details of reconnection are poorly understood, it is well recognized in both astrophysical observations, theory, and in the many fusion confinement experiments that reconnection occurs astonishingly fast, up to Alfvén speed. As a result, physicists concerned with the problem turned to turbulence as the solution, both to produce a small net helicity as well as to produce an enhanced resistivity in order to allow reconnection of the fluxes. Furthermore mean field theory was developed to predict the emergence of large scale fields from the merger of small scale turbulent motions (Steenbeck, Krause & Rädler 1966; Steenbeck & Krause 1969a,b). Ever since, mean field turbulent dynamo theory has dominated the subject for the last 40 years.

1.4. The Turbulent Dynamo

There are two principle problems with turbulent dynamos: first, the difficulty of deriving a net and sufficient helicity from random turbulent motions, and secondly, the ease with which the turbulent motions themselves can be suppressed by the back reaction of the field stress, in this case the multiplied toroidal field (Vainshtein, Parker, & Rosner 1993). Regardless of the source of such turbulence, i.e., the α viscosity (Shakura & Sunyaev 1973), the magneto-rotational instability (Balbus & Hawley 1998) or magnetic buoyancy (Chakrabarti, Rosner, & Vainshtein 1994), the turbulent stress will be small compared to the stress of Keplerian motion. The stress of the magnetic field produced will be limited by the back reaction on this turbulence. As discussed later the back reaction would limit the stress of the dynamo fields to values very much less than the Keplerian stress.

The problem of the origin of reconnection remains, but here turbulence in the disk can help where one needs only assume that the flow of energy in turbulence is always dissipative and that the fraction of magnetic energy dissipated by this turbulence may be very small yet satisfy the necessary reconnection. Secondly, fast reconnection (at near Alfvén speed) in low beta, collisionless plasmas has been modeled (Li et al. 2003; Drake et al. 2003).

We note that we are not considering turbulence as a significant source of helicity in the $\alpha\omega$ dynamo, yet at the same time invoking turbulence in order to enhance reconnection.

1.5. The Astrophysical Consequences

We are attempting to demonstrate that a robust dynamo in an accretion disk, dependent upon a small mass fraction of orbiting stars, becomes a dominant magnetic instability of CMBH formation. To the extent to which this indeed is so and since orbiting stars and Keplerian accretion are universal, then it becomes difficult to avoid the conclusion that the free energy of formation of most CMBHs would be converted into magnetic energy.

In our view the magnetic field, both energy and flux, generated by the black hole accretion disk dynamo presumably powers the jets and the giant magnetized radio lobes. For us both of these phenomena are most likely the on-going dissipation by reconnection and synchrotron emission of force-free helices of wound up strong magnetic field produced by the accretion disk dynamo. (The large scale magnetic flux, as indicated by polarization observations where the correlation length is of order the distance between bright knots, M87, Owen, Hardee & Bignell (1980) is equally demanding of the coherence of the dynamo process.) The electromagnetic mechanism of extraction of angular momentum and energy from the accretion disk has been proposed by Blandford (1976) and Lovelace (1976). Recently, the process of formation of such a force-free helix by shearing of the foot-points of the magnetic field by the rotation of the accretion disk has been considered by Lynden-Bell (1996) and Ustyugova et al. (2000); Li et al. (2001a); Lovelace et al. (2002). The magnetic dynamo in the

disk is the essential part of the whole emerging picture of the formation and functioning of AGNs, closely related to the production of magnetic fields within galaxies, within clusters of galaxies, and the still greater energies and fluxes in the IGM. Black hole formation, Rossby wave torquing of the accretion disk (Lovelace et al. 1999; Li et al. 2000, 2001b; Colgate et al. 2003), jet formation (Li et al. 2001a) and magnetic field redistribution by reconnection and flux conversion, and finally particle acceleration in the radio lobes and jets are the key parts of this scenario (Colgate & Li 1999; Colgate, Li, & Pariev 2001). Finally we note that if almost every galaxy contains a CMBH and that if a major fraction of the free energy of its formation is converted into magnetic energy, then only a small fraction of this magnetic energy, as seen in the giant radio lobes (Kronberg et al. 2001), is sufficient to propose a possible feed back in structure formation and in galaxy formation.

1.6. The Back Reaction Limit and Star-Disk Collisions

The main stream of astrophysical dynamo theory is the mean field theory where an exponential growth of the large scale field is sought, while averaging over small scale motions of the conducting plasma usually regarded as turbulence.

The behavior of turbulent dynamos at the nonlinear stage i.e., back reaction, when one can no longer ignore the Ampere force, is not fully understood and is the process of active investigations (Vainshtein & Cattaneo 1992; Vainshtein, Parker, & Rosner 1993; Field, Blackman, & Chou 1999). However, as it was argued by Vainshtein & Cattaneo (1992), the growth of magnetic fields as a result of the action of the kinematic dynamo should lead to the development of strong field filaments with the diameter of the order of $L/Rm^{1/2}$, where L is the characteristic size of the system and Rm is the magnetic Reynolds number. The field in the filaments reaches the equipartition value much sooner than the large scale field, causing the suppression of the α effect due to the strong Ampere force or back reaction, acting in the filaments. As a result, turbulent $\alpha\omega$ dynamos may be able to account for the generation of the large scale magnetic fields only at the level of $Rm^{-1/2}$ of the equipartition value. Finding the mechanism for producing and maintaining large scale helical flows resulting in a robust α effect is thus very important for the generation of large scale magnetic fields of the order of the equipartition magnitude.

One way of alleviating the difficulty with the early quenching of the turbulent α -dynamo may be a nonlinear dynamo, where the α -effect is maintained by the action of the large-scale magnetic field itself rather than by a small-scale turbulent motions. Such a nonlinear dynamo due to the buoyancy of the magnetic field in a rotating medium was first proposed by Moffatt (1978). As magnetic flux tubes are rising, they expand sidewise to maintain the balance of the pressure with the less dense surrounding gas. This sidewise velocity is claimed to cause the magnetic tube to bend under the action of the Coriolis force.

Calculations of the nonlinear dynamo applied to the Sun was performed by Schmitt (1987) and Brandenburg & Schmitt (1998). A somewhat different mechanism for the radial expansion of

the buoyant magnetic loops (due to the cosmic ray pressure) was proposed in the context of the Galactic dynamo by Parker (1992) and detailed calculations of the resulting mean field theory were performed by Moss, Shukurov & Sokoloff (1999). In this case the matter, cosmic rays, would not fall back to the galaxy surface, but the inertial mass of the cosmic rays is smaller than that of the galactic matter by $\sim 10^{-10}$, again greatly reducing the back reaction limit. The buoyant dynamo can amplify the weak large-scale magnetic field, $B_c \sim \text{Rm}^{-1/2} B_{\text{equi}}$, where B_{equi} is the magnetic field in equipartition with the turbulent energy. However, the buoyant α is a fraction (generally, a small fraction) of the velocity of the buoyant rise of the toroidal magnetic fields, $u_B = C(d/H)^{1/2} v_A$, where d is the radius of a flux tube, H is the half thickness of the disk, v_A is the Alfvén speed, and C is a constant of order unity. For $\text{Rm} \sim 10^{15}$ to 10^{20} in the accretion disk, $B_c \sim 10^{-8}$ to $10^{-10} B_{\text{equi}}$. Alfvén speed will be about 10^{-8} to 10^{-10} of sound speed. As we show below, star-disk collisions lead to a large mass ejected above the disk and therefore result in robust, large scale helical motions of hot gas with the rotation velocity exceeding the sound speed in the disk and, therefore, 10^8 to 10^{10} times faster than the buoyant motions of the magnetic flux tubes. Thus, we can safely neglect the buoyant dynamo in our calculations of the linear stage of star-disk collision driven dynamo.

1.7. Star-Disk Collisions

It has now been long realized that the collisions of stars forming the central part of the star cluster in AGNs with the accretion disk lead to the exchange and stripping (or possibly growth) of the outer envelopes of stars and also, inevitably, a change in the momentum of the stars. This makes an important impact on the dynamics of stellar orbits. Thus the evolution of the central star cluster may contribute to providing accretion mass for the formation of the CMBH and can account for part of the observed emission from AGNs (Syer, Clarke, & Rees 1991; Artymowicz, Lin, & Wampler 1993; Artymowicz 1994; Rauch 1995; Vokrouhlicky & Karas 1998; Landry & Pineault 1998). Zurek, Siemiginowska, & Colgate (1994) considered the physics of plasma tails produced after star-disk collisions (see also Zurek, Siemiginowska, & Colgate 1996). They suggest that emission from these tails may account for the broad lines in quasars. Here we suggest another consequence of stars passing through the accretion disk, the generation of magnetic fields.

For this to happen on a large scale and at the Keplerian back reaction limit requires multiple, repeatable coherent rotation through a finite angle and axial translation of conducting matter well above the disk. We emphasize the importance of an experimental, laboratory demonstration of the rotation and translation of plumes, driven by jets in a rotating frame (Beckley et al. 2003). These laboratory plumes are the analogue of those produced by the star disk collisions, which are the source of the helicity fundamental to this dynamo mechanism.

1.8. The Structure of the Accretion Disk

The near universally accepted view of accretion disks is that based upon the transport of angular momentum by turbulence within the disk. This is the α -disk model, which is also referred to as the Shakura–Sunyaev and to many is the standard model. This model was developed by Shakura (1972), Shakura & Sunyaev (1973), and Novikov & Thorne (1973) and since then it has been widely used for geometrically thin and optically thick accretion disks in moderate to high luminosity AGNs. In this model the viscous transport coefficient is limited by the vertical size of an eddy that can "fit" within the height of the disk, $2H$, and the velocity of the eddy of less than sound speed, c_s , within the disk. Thus the maximum possible viscous transport coefficient, ν_{max} becomes $\nu_{max} < Hc_s$, regardless of what source of turbulence or instability one invokes. The consequence of this limitation is that using the Shakura–Sunyaev formalism, a constant mass flow and the physics of radiation transport, pressure, and surface emission one obtains a disk around a typical CMBH of $10^8 M_\odot$ that has too great a mass thickness at too small a radius, ~ 0.013 pc to be consistent within several orders of magnitude with a generally accepted picture of galaxy formation and angular momentum distribution of a "flat rotation curve" disk. This difficulty has been recognized for some time, (Shlosman & Begelman 1989), motivating the consideration of various alternate transport mechanisms. However, a recent in-depth review of the problem by Goodman (2003) finds no simple solution.

As an alternative solution we have found in recent years that large scale horizontal vortices can be excited within a Keplerian disk by appropriate pressure or angular momentum distributions, closely analogous to Rossby vortices within the disk (Li et al. 2001b). These vortices initially have a horizontal dimension of ~ 2 to $4 H$. One might then ask what is the difference with the truncation of eddy size at the disk height of a turbulent disk and the Rossby vortex disk, because both are truncated initially at the same size. The difference is that the Rossby vortices act coherently and so each vortex, regardless of size acts to transport angular momentum in one direction only, namely radially outwards as compared to turbulence, which is a random walk process. Furthermore the Rossby vortices have a further property of merging leading to larger vortices until $r_{vortex} \simeq R/3$. The transport process is then faster or a transport coefficient that can be larger by the ratio $\nu_{Rossby}/\nu_{turbulence} \simeq r/H \sim 10^4$, thus making feasible an accretion disk that matches the flat rotation curve mass and angular momentum distribution of typical galaxy formation. In addition we also take note of the fact that we have recently suggested that the origin of CMBHs and their correlated power law velocity dispersion can be surprisingly explained by forming the CMBH accretion disk using the Rossby vortex instability mechanism rather than the Shakura–Sunyaev turbulent model (Colgate et al. 2003). This prediction and confirmation by observations as well as the mass thickness problem is sufficiently provoking that to consider the accretion disk dynamo model based solely upon the Shakura–Sunyaev model may be misleading. Fortunately the Rossby vortex instability predicts universally a thinner disk and all disk problems with the dynamo become less difficult. Still, as it is described in a companion paper II (Pariev, Colgate & Finn 2006), star-disk collisions driven dynamo operates at radii $\sim 200r_g$ in the accretion disk, where too high mass

thickness of Shakura–Sunyaev disk is not yet a problem for self-gravity and matching to outside ”flat rotation curve”. Shakura–Sunyaev model is also better developed than Rossby vortex model at present. Hence, in order to minimize the number of speculative assumptions, we proceed with our dynamo model based upon the Shakura–Sunyaev disk model and note the alternate differences when necessary.

This work is arranged as follows: in section 2 we discuss the distribution of stars, in section 3 the structure of the accretion disk, and in section 4 the kinematics of star-disk collisions. Finally, we end with a summary.

2. Star Clusters, and their Distributions

To proceed with the dynamo problem we need to address the following issues:

1. What is the distribution of stars in coordinate and velocity space in the central star cluster of an AGN ?
2. What is the velocity, density and conductivity of the plasma in the disk and in the corona of the disk ?
3. What is the hydrodynamics of the flow resulting from the passage of the star through the disk ?

Each of these problems is difficult to solve. Moreover, there are no detailed solutions to these problems up to date. Furthermore they all interrelate. In the following three subsections we present a brief (far from complete) analysis of each of the problems based on available research and some of our own conjectures. Because each of these problems interrelate to some degree with each other, the justification of some assumptions must be delayed. However, as noted above, we will predict a dynamo gain so large that details of the disk and of the star disk collisions and their frequency become of secondary importance compared to the existence of the disk, a few stars and the CMBH.

2.1. Kinematics of the Central Star Cluster

By now there is strong observational evidence (e.g., Tremaine et al. 2002; Merritt & Ferrarese 2001; van der Marel 1999; Kormendy et al. 1998; van der Marel et al. 1997) that many galactic nuclei contain massive dark objects in the range of $\approx 10^6 - 10^9 M_{\odot}$. Numerical simulations of the evolution of central dense stellar clusters indicate that they are unstable to the formation of black holes, which would subsequently grow to larger masses by absorbing more stars (Quinlan & Shapiro 1990). Recent observations and the interpretation of very broad skewed profiles of iron emission line (e.g., Tanaka et al. 1995; Bromley, Miller, & Pariev 1998; Fabian et al. 2000) in

Seyfert nuclei provide direct evidence for strong gravitational effects in the vicinity of massive dark objects in AGNs. This leaves us with conviction that the nuclei of AGNs indeed harbor black holes with accretion disks (Fabian et al. 1995). Although the observations of star velocities and velocity dispersion are used to obtain an estimate of the mass of the supermassive black hole, a measurement of the number density of stars is limited by resolution to about 1 pc for M32 and M31 and about 10 pc for the nearest ellipticals. From these observations we infer a star density of $n(1 \text{ pc}) \approx 10^4 - 10^6 M_\odot \text{pc}^{-3}$ at 1 pc (Lauer et al. 1995).

One needs to rely on the theory of the evolution of the central star cluster in order to obtain number densities of stars closer to the black hole. The subject of the evolution of a star cluster around a supermassive black hole has drawn significant interest in the past. The gravitational potential inside of the central 1 pc will be always dominated by the black hole. Bahcall & Wolf (1976) showed that, if the evolution of a star cluster is dominated by relaxation, the effect of a central Newtonian point mass on an isotropic cluster would be to create a density profile $n \propto r^{-7/4}$. However, for small radii ($\approx 0.1 - 1 \text{ pc}$) the effects of physical collisions between stars become dominant over two-body relaxation. Also, the disk produces a drag on the stellar orbits, which accumulates over many star passages. The result of the star-disk interactions is to reduce the inclination, eccentricity, and semimajor axis of an orbit, finally causing the star to be trapped in the disk plane, and so moving on circular Keplerian orbits (Syer, Clarke, & Rees 1991; Artymowicz, Lin, & Wampler 1993; Artymowicz 1994; Rauch 1995; Vokrouhlicky & Karas 1998). Closer to the black hole ($\leq 100r_g$, $r_g = 2GM/c^2$, the gravitational radius) general relativistic corrections to the orbital motions and tidal disruption of the stars by the black hole must be taken into account. Considering all these effects and furthermore that the star-star collisions cannot be treated in a Fokker–Plank (or diffusion) approximation, an accurate theory becomes a difficult endeavor, which has not yet been completed to our knowledge.

To obtain a plausible estimate of the number density and velocity distribution of stars in the central cluster we will follow the work of Rauch (1999), which addresses all these effects on the star distribution mentioned above, except the dragging by the disk. Rauch (1999) showed that star-star collisions lead to the formation of a plateau in the density of stars for small r because of the large rates of destruction of stars by collisions. We adopt the results of model 4 from Rauch (1999) as our fiducial model. This model was calculated for all stars having initially one solar mass. The collisional evolution in model 4 are close to the stationary state, when the combined losses of stars due to collisions, ejection, tidal disruptions and capture by the black hole are balanced by the replenishment of stars as a result of two-body relaxation in the outer region with $n \propto r^{-7/4}$ density profile. Taking into account the order of magnitude uncertainties in the observed star density at 1 pc, the fact that model 4 has not quite reached a stationary state can be acceptable for the purpose of order of magnitude estimates.

For the mass of the black hole we take $M = 10^8 M_8 M_\odot$. The radius of the event horizon of the black hole is $r_g = 2GM/c^2 = 3.0 \cdot 10^{13} \cdot M_8 \text{ cm} = 9.5 \cdot 10^{-6} \cdot M_8 \text{ pc}$. We then approximate the

density profile of model 4 as

$$\begin{aligned}
 n &= n_5 \cdot 10^5 \frac{M_\odot}{\text{pc}^3} \left(\frac{r}{1\text{pc}} \right)^{-7/4} && \text{for } r > 10^{-2} \text{ pc}, \\
 n &= n_5 \cdot 3 \cdot 10^8 \frac{M_\odot}{\text{pc}^3} && \text{for } 10r_t < r < 10^{-2} \text{ pc}, \\
 n &= 0 && \text{for } r < 10r_t,
 \end{aligned} \tag{1}$$

where $r_t = 2.1 \cdot 10^{-4} \text{ pc} \cdot M_8^{1/3} = 21r_g$ is the tidal disruption radius for a solar mass star, $n_5 = \frac{n(1 \text{ pc})}{10^5 M_\odot/\text{pc}^{-3}}$, $M_8 = M/10^8 M_\odot$. An integration of expression (1) over volume produces the number of stars with impact radii inside a given radius, $N(< r)$, as:

$$\begin{aligned}
 N(< r) &= n_5 \cdot \left[10^6 \left(\frac{r}{1\text{pc}} \right)^{5/4} - 1.9 \cdot 10^3 \right] && \text{stars for } r > 10^{-2} \text{ pc}, \\
 N(< r) &= n_5 \cdot 12 \left[\left(\frac{r}{10r_t} \right)^3 - 1 \right] && \text{stars for } 10r_t < r < 10^{-2} \text{ pc}, \\
 N(< r) &= 0 && \text{stars for } r < 10r_t,
 \end{aligned} \tag{2}$$

such that $N(< 10^{-2} \text{ pc}) = 1.3 \cdot 10^3 n_5$ stars. Thus in this conservative view there are no star disk collisions and therefore no dynamo inside $200r_g$. One notes that the total mass of stars inside central 0.1 pc remains a small fraction ($< 10^{-2}$) of CMBH mass.

This extrapolated lack of stars within the inner most regions of the disk presumably occurs because of star-star collisions and tidal disruption of stars and is independent of disk structure. The zero n at $r < 10r_t$ is a crude approximation to actual decrease in the number density of stars. This is because we recognize that distant gravitational scattering will lead to some diffusion of stars from distant regions and thus feeding of stars to the inner regions, limited by r_t .

We shall comment further on the influence of the drag by the disk on the above density profile. Following the formula [1] from Rauch (1999) the probability that the solar mass star on the elliptic orbit with eccentricity e and the minimum distance from the black hole r_{min} will experience a collision with another star during one orbital period is

$$\tau_{coll} = 2 \cdot 10^{-5} \cdot n_5 M_8^{-3/4} (3 - e) \left(\frac{r_{min}}{r_g} \right)^{-3/4}. \tag{3}$$

This probability at $100r_g$ or $\sim 10^{-3} \text{ pc}$ becomes

$$\tau_{coll} = 6 \cdot 10^{-7} \cdot n_5 M_8^{-3/4} (3 - e). \tag{4}$$

This probability is sufficiently small that the drag of the disk during star-disk collisions can be more important. In order to evaluate that drag we need to know the surface density in the disk.

3. Disk Structure and Star Collisions

We adopt the α -disk model, which we also refer to as the Shakura–Sunyaev (Shakura 1972; Shakura & Sunyaev 1973) model. We also consider the Rossby vortex model for reasons outlined in the introduction. As noted before, fortunately the Rossby vortex instability predicts universally a thinner disk and all disk problems with the dynamo become less difficult. Hence we proceed with our dynamo model based upon the Shakura–Sunyaev disk model and note the alternate differences when necessary.

For thirty years, the Shakura–Sunyaev disk model has been the most widely used model of the accretion disk. The expressions for the parameters of the α -disk can be found in original articles (Shakura 1972; Shakura & Sunyaev 1973) and in many later books (e.g., Shapiro & Teukolsky 1983; Krolik 1999; Bisnovatyi-Kogan 2002). Here, we give the complete set of these expressions conveniently scaled for our problem (supermassive black hole, radius about $200r_g$ or 10^{-2} pc) in Appendix A.

There have been a number of works perfecting and improving the simple analytical Shakura–Sunyaev model and determining the limits of applicability of this solution to real AGN accretion disks. Here we leave aside the complex physics of the innermost ($\leq 10r_g$) parts of the accretion flow because the innermost regions are devoid of stars and so star-disk collisions are almost non-existent in this region. More realistic bound-free opacities were included by Wandel & Petrosian (1988), non-LTE models were developed by Hubeny & Hubeny (1997, 1998) in disks with arbitrary optical depth, and optically thin and optically thick disks, were considered in Artemova et al. (1996). If one is looking at the interval of disk radii ~ 100 to $\sim 1000r_g$, these improvements have some quantitative effects on the disk structure such as the emitted spectrum may be significantly different among models. More exact descriptions of the accretion disk come at a price of losing analytic simplicity of the expressions for the radial profiles of the density, temperature, disk height, etc., while gaining a factor of only a few in accuracy. Because of the approximate nature of our model (mandated by the poor accuracy of its other ingredients), we prefer to use the simplest of the disk models, and therefore use the analytic results given in the original works of Shakura and Sunyaev.

The surface density of the α -disk in the inner radiation dominated part, where Compton opacity prevails, is given by expression (A4) in the Appendix A. When expressed in units of M_\odot/R_\odot^2 , it becomes

$$\Sigma = 9.9 \cdot 10^{-10} \frac{M_\odot}{R_\odot^2} \left(\frac{\alpha_{ss}}{0.01} \right)^{-1} \left(\frac{l_E}{0.1} \right)^{-1} \left(\frac{\epsilon}{0.1} \right)^1 \left(\frac{rc^2}{GM} \right)^{3/2} \left(1 - \sqrt{\frac{3r_g}{r}} \right)^{-1}, \quad (5)$$

where α_{ss} is the “ α ”-parameter of the disk model, l_E is the ratio of the luminosity of the disk to the Eddington limit for the black hole of mass M , ϵ is the fraction of the rest mass energy of the accreting matter, which is radiated away. Thus close to r_g , $\Sigma = 404 \text{ g cm}^{-2}$. The expression (5) is valid for a radiation pressure supported disk where $r < r_{ab}$ given by expression (A2). For

typical values $\alpha_{ss} = 0.01$, $\epsilon = 0.1$, $l_E = 0.1$, $M_8 = 1$, we obtain $r_{ab} = 2.3 \cdot 10^{-3} \text{ pc} \approx 240r_g$ and $\Sigma_{ab} = \Sigma(r_{ab}) \approx 4.2 \cdot 10^6 \text{ g cm}^{-2}$.

When the disk becomes self gravitating, it may become subject to a gravitational instability. In Appendix A we check that by calculating the Toomre parameter $\text{To} = \frac{\varkappa c_s}{\pi G \Sigma}$ (e.g., Binney & Tremaine 1994), where \varkappa is the epicyclic frequency and c_s is vertically averaged sound speed. The gravitational instability develops if $\text{To} < 1$. As follows from the analysis in the Appendix A the disk has a well defined radius of stability r_T , such that for $r > r_T$ it becomes unstable. In the case when $r_T < r_{ab}$, the expression for r_T is given by formula (A33). For the values $\alpha_{ss} = 0.01$, $\epsilon = 0.1$, $l_E = 0.1$, $M_8 = 1$ the radius of stability r_T falls close to the radius of transition r_{ab} between radiation dominated and gas pressure dominated parts of the disk. The development of the Jeans instability should lead to the formation of spiral patterns and fragmentation of the disk (Shlosman & Begelman 1989), which will happen on the radial inflow time scale at a radius $\approx r_T$. Therefore, for estimating the drag produced by the disk on the passing stars, we can limit ourselves to consider only the inner portion of the disk at $r < r_{ab}$ and use equation (5) for the disk surface density. The gas beyond r_{ab} may also influence the motion of stars. It is difficult to evaluate the drag produced on stars passing through gravitationally unstable outer parts of the disk for $r > r_T$. However, we note that the rate of star-disk collisions is maximized at $r \lesssim 10r_t \sim r_{ab}$, so most of the star-disk collisions happen inside the radiation dominated zone (zone (a)) of the disk.

The Rossby vortex model of the disk predicts a mass thickness of a near constant, $100 \text{ g cm}^{-2} < \Sigma_{RVI} < 1000 \text{ g cm}^{-2}$. This is about the same as the Shakura–Sunyaev model near to the BH, but becomes very much less at large radius. Consequently the self gravity condition occurs at a much larger radius, 3 to 10 pc, and matches smoothly onto the galactic flat rotation curve mass distribution.

Hereafter, we will use disk parameters in zone (a) listed in Appendix A for the estimates of star-disk collisions. The disk half-thickness (expression (A5)) expressed in units of r_g is

$$H = 1.15 \cdot r_g \left(\frac{l_E}{0.1} \right) \left(\frac{\epsilon}{0.1} \right)^{-1} M_8 \left(1 - \sqrt{\frac{3r_g}{r}} \right), \quad (6)$$

expressed in solar radii

$$H = 370 R_\odot \left(\frac{l_E}{0.1} \right) \left(\frac{\epsilon}{0.1} \right)^{-1} M_8 \left(1 - \sqrt{\frac{3r_g}{r}} \right), \quad (7)$$

and expressed as a fraction of r_{ab}

$$H = 3.7 \cdot 10^{-3} r_{ab} \left(\frac{\alpha_{ss}}{0.01} \right)^{-2/21} \left(\frac{l_E}{0.1} \right)^{5/21} \left(\frac{\epsilon}{0.1} \right)^{-5/21} M_8^{-2/21} \left(1 - \sqrt{\frac{3r_g}{r}} \right). \quad (8)$$

It is natural to expect that the dynamo growth rate will be also maximized at small radii primarily within zone (a) where the disk is radiation dominated, but outside of the region, $r_t \simeq 21r_g$,

of tidal destruction of stars. However, we should also point out that although proof of principle of the dynamo is most likely where the growth rate is maximum, we also expect that regardless of where the growth rate maximizes, that the back reaction will limit the maximum fields and that subsequent diffusion outwards (as for the angular momentum) and advection inwards (as for the mass) will ensure a redistribution of the magnetic flux reaching a new equilibrium presumably less dependent upon where the maximum dynamo growth rate occurs.

3.1. Star-Disk Interaction

The orbital period of the star is

$$t_{orb} = 3.1 \cdot 10^3 \text{ s} \cdot M_8 \left(\frac{r_{min} c^2}{GM} \right)^{3/2} (1 - e)^{-3/2}. \quad (9)$$

where, as before, r_{min} is the minimum impact radius of the star's orbit. The typical velocity of the star relative to the disk is close to the Keplerian velocity at r_{min} . Since the speed of sound in the disk is much smaller than the Keplerian velocity, by the ratio $H/r \simeq 3.7 \cdot 10^{-3}$, stars pass through the disk with highly supersonic velocities. The drag force on the star consists of two components, collisional and gravitational. The collisional or direct drag is produced by intercepting the disk material by the geometric cross section of the star. Assuming the star to have a solar mass and radius, this force is $F_{drag} = \pi R_\odot^2 \rho v_*^2$, where ρ is the mass density of the gas in the disk, and v_* is the velocity of the star relative to the disk gas. Radiation drag is negligible compared to gas drag as soon as the speed of sound is nonrelativistic, i.e. $c_s \ll c$. The second component of the drag force is due to deflection of the gas by the gravitational field of the star. Rephaeli & Salpeter (1980) found that the latter component is nonzero only for supersonic motion and gave the following expression for that force in the limit $v_* \gg c_s$

$$F_{grav} = 4\pi \frac{G^2 M_\odot^2}{v_*^2} \rho \ln \Lambda, \quad (10)$$

where Λ is the Coulomb logarithm. The ratio of the two forces is

$$\frac{F_{drag}}{F_{grav}} = \frac{R_\odot^2 v_*^4}{G^2 M_\odot^2 4 \ln \Lambda}. \quad (11)$$

Using for v_* its Keplerian value $v_* = (GM/r)^{-1/2}$, and using for the Coulomb logarithm its maximum possible value $\Lambda = r/R_\odot$, one obtains the ratio of the forces as

$$\frac{F_{drag}}{F_{grav}} = \frac{1.03 \cdot 10^{10}}{1 + 0.19 \ln(M_8 \frac{c^2 r}{GM})} \left(\frac{GM}{c^2 r} \right)^2. \quad (12)$$

One can see from equation (12) that the force due to the direct interception of gas by the star is much larger than the drag caused by the gravitational drag for all values of r of interest

to us $r \lesssim 10^5 r_g$. Thus, we can consider the change of momentum caused by the disk on passing stars as purely due to the interception of the gas by the geometrical cross section of the star πR_\odot^2 . Hence, the characteristic time needed to substantially change the star orbit as a result of star-disk interactions, t_{disk} , is approximately equal to the time needed for the star to intercept the disk mass equal to the mass of the star. A star will pass through the disk twice per one orbital period. Assuming all stars as having a solar mass and radius, the ratio of the orbital period to t_{disk} is

$$\tau_{disk} = \frac{t_{orb}}{t_{disk}} \approx \frac{2\Sigma\pi R_\odot^2}{M_\odot}.$$

Using expression (5) for Σ in the region $r < r_{ab}$ one obtains

$$\tau_{disk} = 6.2 \cdot 10^{-9} \left(\frac{\alpha_{ss}}{0.01}\right)^{-1} \left(\frac{l_E}{0.1}\right)^{-1} \frac{\epsilon}{0.1} \left(\frac{c^2 r_{min}}{GM}\right)^{3/2} \left(1 - \sqrt{\frac{3r_g}{r_{min}}}\right)^{-1}. \quad (13)$$

The corresponding star-disk interaction time scale t_{disk} is given by

$$t_{disk} = 1.58 \cdot 10^4 \text{ yr} \cdot \frac{\alpha_{ss}}{0.01} \frac{l_E}{0.1} \left(\frac{\epsilon}{0.1}\right)^{-1} M_8^{-1/2} \frac{1}{(1-e)^{3/2}} \left(1 - \sqrt{\frac{3r_g}{r_{min}}}\right), \quad (14)$$

and is independent of the semi-major axis of the star orbit. As was shown by Rauch (1995) secular evolution of all orbital elements of a star happen at the same time scale t_{disk} from equation (14). The ratio of τ_{disk} to τ_{coll} (equation (3)) is given by

$$\frac{\tau_{disk}}{\tau_{coll}} = 1.8 \cdot 10^{-4} n_5^{-1} \frac{1}{3-e} M_8^{3/4} \left(\frac{\alpha_{ss}}{0.01}\right)^{-1} \left(\frac{l_E}{0.1}\right)^{-1} \left(\frac{\epsilon}{0.1}\right)^1 \left(\frac{c^2 r}{GM}\right)^{9/4} \left(1 - \sqrt{\frac{3r_g}{r_{min}}}\right)^{-1}. \quad (15)$$

For orbits with $r_{min} \leq 30r_g$ one has $\tau_{disk} < \tau_{coll}$ and the effect of star-disk collisions dominates over the effect of star-star collisions (assuming typical parameters for the disk). For the radii $30r_g \leq r_{min} \leq r_T$ the orbit evolution is more influenced by the drag from the disk rather than by star-star collisions. (We note that this radius, $30r_g$, is only slightly greater than the gravitational disruption radius by the CMBH, $r_t \simeq 20r_g$.) Only a fraction of stars from the outer region located beyond $\approx 1000r_g$ will not be put into the disk plane by star-disk drag. Results of Rauch (1995) show that it takes a considerably longer time than t_{disk} to reorient the retrograde star orbits. During this reorientation process the semimajor axes of initially retrograde star orbits decreases by ≈ 10 times. Before the alignment process for such stars could be completed they will move in radius closer than $\approx 30r_g$ into the star-star collisions zone, where their orbital inclinations would be randomized. Another factor preventing all stars from being trapped into the disk plane is that there is always a fraction of stars which are injected by two body relaxation into the neighborhood of the black hole from large (much larger than r_T) radii. These stars can be brought directly into the region $r \leq 30r_g$ (or close to it) and contribute to the collisional core of the stellar cluster.

To summarize, both star-disk and star-star collisions can be important for determining the distribution function in the central star cluster. However, it seems unlikely that the drag by the disk can trap all stars into the disk plane and denude the central $\approx 10^{-3}$ pc of all stars not in the

disk plane. Trapping of stars by the disk will reduce the numbers of stars given by (1) but this requires more evolved computations, which are beyond the scope of the present work. Both star-star collisions and the effect of trapping by the disk of the stars having lower eccentricities faster than the stars having larger eccentricities leads to highly eccentric orbits of stars in the central $\approx 10^{-3}$ pc. Drag by the disk will also lead to the prevailing of prograde orbits over the retrograde orbits. However, for our purpose, we assume that the star density is given by equations (1), all stars have $e = 1$ and their orbits are randomly oriented in space. (This approximation is better in the model of the disk driven by Rossby vortices.)

3.2. The Rate of Star-Disk Collisions

We shall use the number density of stars, n , given by equation (1) in order to evaluate the rate of star-disk collisions. The flux of stars through the disk coming from one side of it is $nv/4$, where we assume that all stars have the same velocity $v = \sqrt{2}(r\Omega_K)$ (parabolic velocity) and are distributed isotropically. One obtains then for $M_8 = 1$

$$\begin{aligned} \frac{1}{4}nv &= 2.4 \cdot 10^{-39} \frac{1}{\text{cm}^2\text{s}} n_5 \left(\frac{r}{10^{-2} \text{ pc}} \right)^{-9/4} && \text{for } r > 10^{-2} \text{ pc}, \\ \frac{1}{4}nv &= 2.4 \cdot 10^{-39} \frac{1}{\text{cm}^2\text{s}} n_5 \left(\frac{r}{10^{-2} \text{ pc}} \right)^{-1/2} && \text{for } 10r_t < r < 10^{-2} \text{ pc}, \\ \frac{1}{4}nv &= 0 && \text{for } r < 10r_t. \end{aligned} \quad (16)$$

Integrating the flux of stars coming from both sides of the disk over an area of πr^2 inside some given radius r , one can estimate the rate of star-disk collisions within the radius r . Let us define the time $\Delta T_c = \Delta T_c(r)$ as the inverse of this rate, i.e. one star passes through the disk area inside the radius r during the time ΔT_c on average. The result is (see equation (1))

$$\begin{aligned} \Delta T_c &= \frac{2\pi}{\Omega_K(r)} \cdot 2.8 \cdot 10^{-5} \cdot n_5^{-1} \left(\frac{r}{10^{-2} \text{ pc}} \right)^{-3/2} && \text{for } r > 10^{-2} \text{ pc}, \\ \Delta T_c &= \frac{2\pi}{\Omega_K(r)} \frac{1.9 \cdot 10^{-2}}{n_5 \left(\frac{r}{10r_t} \right)^{3/2} \left(\left(\frac{r}{10r_t} \right)^{3/2} - 1 \right)} && \text{for } 10r_t < r < 10^{-2} \text{ pc}, \\ \Delta T_c &= \infty && \text{for } r < 10r_t \text{ (no collisions),} \end{aligned} \quad (17)$$

where $2\pi/\Omega_K(r) = T_K(r)$ is the period of Keplerian circular orbit at the radial distance r from the black hole. We see that the number of star-disk collisions happening per Keplerian period, $T_K(r)$, is $\propto r^3$ inside the collisional core of the star cluster, e.g. within $\approx 10^{-2}$ pc. For the outer region of the stellar cluster beyond $\approx 10^{-2}$ pc this number continues to increase with r but more slowly, as $\propto r^{3/2}$. The number of collisions per Keplerian period at 0.01 pc is $\sim 30,000$, leading to fluctuations of the order of 1% within an orbital time of several years.

If these collisions should produce broad emission and absorption lines regions, (BLRs), then this result may not be inconsistent with observations. Estimates of the density of the matter leading to the broad emission lines from the interpretation of allowed and forbidden transitions give a density of $\rho_{BL} \sim 10^{-11}$ to 10^{-13} g/cm³, (Sulentic, Marziani & Dultzin-Hacyan 2000). The geometrical thickness of the disk H in radiative pressure dominated inner zone is independent of the disk model and the mechanism of angular momentum transport and is given by equation (A5). In thermal pressure dominated part of the disk, H weakly depends on Σ as $H \propto \Sigma^{1/8}$. Only in the case of the RVI disk does the low thickness, $\Sigma_{RVI} \sim 10^2$ to 10^3 g/cm³, lead to a sufficiently low density, $\rho_{RVI} = \Sigma_{RVI}/H \simeq \Sigma_{RVI} \cdot 3 \cdot 10^{-14}$ g/cm³, which is consistent with the above estimates for the density of the star-disk driven matter emitting the broad emission lines. On the other hand, the Shakura–Sunyaev disk would be expected to have a density ρ_{SS} given by expression (A6) in the radiation dominated zone (a) and expression (A25) in the pressure dominated zone (b). If one equates the observed width of broad emission lines ($\sim 7 \cdot 10^3$ km/s) to the Doppler shift at Keplerian velocity, one obtains an estimate of the location of the broad lines region at $r \sim 10^3 r_g$. This radius falls not far from the boundary between zones (a) and (b) in the Shakura–Sunyaev disk model (see expression (A2)). The density of the Shakura–Sunyaev disk at this radius is $\sim 10^{-6}$ g/cm³ to 10^{-8} g/cm³ depending upon the parameters of the model. This is at least 5 orders of magnitude larger than ρ_{BL} required by observations. The differences in ρ for Shakura–Sunyaev and RVI disks are almost completely attributable to the much lower column thickness Σ_{RVI} than Σ for Shakura–Sunyaev model. Regardless, the function of the plumes for producing the helicity for the dynamo should be independent of these differences in the models of the disk.

Star disk collisions were first suggested as the source of the BLRs by Zurek, Siemiginowska, & Colgate (1994), Zurek, Siemiginowska, & Colgate (1996), but a detailed calculation of the phenomena has not yet been performed, because it requires 3-D hydrodynamics with radiation flow and opacities determined by multiple lines. An approximation to this problem was calculated by Armitage, Zurek & Davies (1996) for the purpose of determining the mass accretion rate of giant stars by dynamic friction with the disk, but the radiation flow in thin disks was not considered. We recognize that very many additional variables of hydrodynamics, radiation, and geometry must be taken into account in order to positively identify BLRs with star disk collisions. With these caveats we proceed to analyze the star collisions with the disk and the resulting plume formation from the standpoint of the fluid dynamics that has consequences for the dynamo.

4. Plumes Produced by Star Passages through the Disk

The first result of a star-disk collision is to cause a local fraction of the mass of the disk to rise above the surface of the disk because of the heat generated by the collision. Two plumes expanding on both sides of the accretion disk will be formed. A second result is the expansion of this rising mass fraction relative to its vertical axis in the relative vacuum above the disk surface and again because of the internal heat generated by the collision. A third result is the rotation (anticyclonic) of this

expanding matter relative to the Keplerian frame corotating with the disk because of the Coriolis force acting on the expanding matter. Again we emphasize that this rotation through a finite angle has been measured in the laboratory and agrees with a simple theory of conservation of angular momentum and radial expansion of the plume (Beckley et al. 2003). All three effects are important to the dynamo gain. However, we will find that the dynamo gain during the life time of the accretion disk, $\sim 10^8$ years, is so large that the accuracy of the detailed description of these "plumes" becomes of less importance compared to the facts of: (1) their axial displacement well above the disk; (2) their finite, $\sim \pi/2$ radians, coherent rotation every star-disk collision; and (3) their subsidence back to the disk in $\sim \pi$ radians. In this spirit we will estimate the hydrodynamics of the star-disk collision, attempting to establish the universality of this phenomena as the basis of the accretion disk dynamo. As far as we know no hydrodynamic simulations of the behavior of the disk matter due to stars passing through the disk have yet been performed. (This is because of the difficulty of 3-dimensional hydrodynamics with radiation flow.) The star passes through the disk at a velocity, close to the Keplerian velocity of the disk at whatever radius the collision happens. The sound speed in the accretion disk is much less than the Keplerian speed v_K : $c_s \simeq v_K H/r \simeq 3 \cdot 10^{-3} v_K$ at r_{ab} , where H is the disk half-thickness given by expression (A5) in zone (a). Hence, the star-disk collisions are highly supersonic. The temperature of the gas in the disk, shocked by the star moving at a Keplerian velocity, is of the order of the virial temperature in the gravitational potential of the central black hole. This pressure must include the radiation contribution, which in general, will be much larger than the particle pressure. Because of the high Mach number of the collision, the pressure of the shocked gas is very much greater than the ambient pressure in the disk. This over pressure will cause a strong, primarily radial shock, radial from the axis of the trajectory, in the wake of the star, because of the large, length to diameter ratio of the hot channel, $H/R_\odot \simeq 4 \cdot 10^2$. After the star emerges above the disk surface (i.e. higher than the half thickness of the disk), the heated shocked gas in the wake of the star continues to expand sideways and furthermore starts to expand vertically because of the rapidly decreasing ambient pressure away from the disk mid-plane where the pressure of the disk drops as $\propto \exp(-z^2/H^2)$. Thus this expansion can be treated as an adiabatic expansion into vacuum after the plume rises by a few heights H above and below the disk, provided the radiative loss is fractionally small. We would now like to estimate the size, or radius, r_p , of the matter that rises $\sim 2H$ above the disk, or to a height $l \simeq 3H$ above the mid-plane. Although smaller mass fractions with greater internal energy corresponding to smaller radii of the shock will expand to greater heights above the disk, nevertheless we are concerned with only this modest height, because we expect that the mass and hence entrained magnetic flux to be positively correlated with plume mass, and we wish to maximize the entrained flux. On the other hand, by conservation of energy, a larger mass will rise or expand to a smaller height. We also desire the plume to rise sufficiently above the disk such that there is ample time for radial expansion and hence torquing of the entrained magnetic field during the rise and fall of the plume material. This will be our standard plume.

The radial extend of the plume should be somewhat less than its vertical extend because the density gradient in the disk is largest in the vertical direction. The action of the Coriolis force

leads to an elliptical shape of the horizontal cross section of the plume. This is due to the fact that epicycles of particles in the gravitational field of a point mass are ellipses with an axis ratio of 2 and with an epicyclic frequency of Ω_K . We performed simple ballistic calculations of trajectories of particles launched from a point at the mid-plane of the disk with initial velocities in different directions in the horizontal plane. We obtained that at the time of maximum height of the plume, $\approx T_K/4$, the position angle of the major axis of the ellipse is approximately $-\pi/4$ from the outward radial direction \mathbf{e}_r . At the time of the fall back to the disk plane at $\approx T_K/2$, the major axis of the ellipse is close to the azimuthal direction. Such a distortion in the shape of an otherwise cylindrical plume will only slightly affect the rotation of the entrapped toroidal flux and hence will not alter the dynamo action.

Before calculating the size or radius, r_p , we first verify the adiabatic approximation in that the diffusion of radiation is fractionally small compared to the hydrodynamic displacements. In this circumstance of a Shakura–Sunyaev disk, this will allow us to treat the star-disk collisions as strong shocks within the disk matter. Subsequently we will consider the thinner, lower density Rossby disks (Li et al. 2001b) where radiation transport will dominate over shock hydrodynamics. However, for the purposes of the dynamo, the production of helicity from either plumes will be similar.

4.1. Radiation Diffusion in the Collision Shock

During star-disk collisions the total energy taken from the star is $\approx \Sigma v_K^2 \pi R_\odot^2$. This energy is distributed over a column of radial extent, ΔR_{rad} , due to radiation transport. For an estimate of ΔR_{rad} one can take the distance from the star track where the sideways diffusion of radiation becomes comparable with the advection of the radiation by the displacement of the disk matter with the star velocity v_K (since the velocity of strong shock is of the order of v_K). This results in

$$\Delta R_{rad} = \frac{c/3}{\kappa \rho v_K}, \quad (18)$$

where for ρ we consider the density ahead of the shock in the undisturbed disk matter to compare the radiation flux with the transport of energy and momentum by the shock. We assume $\kappa = 0.4 \text{ cm}^2 \text{ g}^{-1}$, Thompson opacity. Then using ρ from expression (A6) at r_{ab} ,

$$\Delta R_{rad} = 10^8 \text{ cm} = 1.4 \cdot 10^{-3} R_\odot. \quad (19)$$

Since $\Delta R_{rad} \ll R_\odot$, the radiation will remain local to the shocked fluid. The state conditions in this shocked matter will depend upon the rapid thermalization between the matter and radiation.

The number of photon scatterings, $n_{h\nu}$ within the time of traversal of the radiation front, ΔR_{rad} , becomes

$$n_{h\nu} = (\Delta R_{rad} \kappa \rho)^2 = \left(\frac{c/3}{v_K} \right)^2 = 50 \left(\frac{r}{r_{ab}} \right). \quad (20)$$

Therefore the radiation will be fully absorbed and thermalized with the gas within ΔR_{rad} . Since the gas pressure is radiation dominated for $r < r_{ab}$ and the shock has a high Mach number, $c_s/v_K \approx r/H \simeq 280$ at r_{ab} , then the shocked matter will have a still higher entropy and be even further radiation dominated. In a strong shock the energy behind the shock will be half kinetic and half internal energy, where in this case the radiation pressure dominates. Thus the subsequent evolution of the radiation dominated gas will be governed by adiabatic hydrodynamics of the fluid with a polytropic index $\gamma = 4/3$.

4.2. The Shock Produced by the Collision and Its Radial Expansion

Since the initial radius of the shocked gas is that of the star and since this radius is small compared to the path length through the disk, H , or $H/R_\odot \approx 370$ at $r = r_{ab}$, we make the assumption that the collision can be approximated as a line source of energy with the energy deposition per unit length $\Sigma v_K^2 \pi R_\odot^2$, and consider the shock wave as expanding radially from the trajectory axis. This can be well described as one of the sequence of Sedov solutions (Sedov 1959) of an expanding cylindrical shock in a uniform medium. However, for the purposes of the accuracy required for our plume approximation it is sufficient to note that the energy density left behind the shock, ϵ_{shk} , is nearly inversely proportional to the swept-up mass, or $\epsilon_{shk} \simeq \epsilon_{shk,R_\odot} (R_\odot/R_{shk})^2$ where $\epsilon_{shk,R_\odot} \simeq v_K^2/2$. This increase in energy density leads to an increase in the pressure of the shocked gas P_{shk} relative to the ambient pressure P_o : $P_{shk,R_\odot}(z) \simeq \rho v_K^2 \gg P_o(z)$ for all z . The high pressure of the shocked gas near the axis of the channel will drive the shock to larger radii while expanding adiabatically behind the shock. Near the surface, $R_{shk} \simeq z$ the shocked gas can expand vertically as well as horizontally. However, to the extent that when the shock is strong, $R_{shk} \ll H$, the radial shock will have decreased in strength before the star reaches the surface and the over pressure becomes too small except for a small mass fraction of the surface mass, $\Delta z \simeq R_{shk} \ll H$, that will expand vertically above the disk surface.

However, a larger mass will expand above the disk due to buoyancy. In this case the vertical momentum is derived primarily from the difference of gravitational forces on the buoyant matter versus the ambient matter. The buoyant force is proportional to the entropy ratio. A strong shock leaves behind matter whose entropy is higher than the ambient medium. Since the entropy change due to a shock wave is third order in the shock strength (Courant & Friedrichs 1948; Zeldovich & Raizer 1967), only strong shocks result in significant changes in entropy. In this limit the entropy change ΔS from the ambient entropy S_o is $\Delta S/S_o \propto \Delta(P/\rho)/(P_o/\rho) \simeq (P_{shk}/P_o)((\gamma - 1)/(\gamma + 1))$ where γ is the usual ratio of specific heats, and ρ is the ambient density. The compression ratio is $\eta_{CR} = \rho_{shk}/\rho = (\gamma + 1)/(\gamma - 1) = 7$ across a strong shock for $\gamma = 4/3$. Thus, for example, for a plume to rise well above the disk requires an estimated $\Delta S/S_o \geq 2$ and thus $P_{shk}/P_o \simeq 14$. Once the hot shocked gas rises to the surface of the disk and assuming that this flow is adiabatic thereafter and thus does not entrain a significant fraction of surrounding matter, the subsequent expansion above the disk is determined by its initial internal energy.

Let us consider the neighborhood of a point $r = r_0$ at the mid-plane of the disk where a star disk collision occurs. One can introduce a local Cartesian coordinate system x, y, z in the Keplerian rotating frame with the origin at the point $r = r_0$ such that the x -axis is directed radially outward, the y -axis is directed in the positive azimuthal direction, and the z -axis is perpendicular to the disk plane. Then, the effective gravitational and centrifugal potential in the Keplerian rotating frame in the neighborhood of the point $r = r_0$ is

$$\Delta\Phi = \frac{GM}{2r_0^3}(z^2 - 3x^2). \quad (21)$$

The thermal energy of the hot column of gas is a fraction of the loss of kinetic energy of the star due to the hydrodynamic collision with the disk. This latter energy loss during one passage is $F_{drag}2H = 2H\pi R_\odot^2 \rho v_*^2 = \pi R_\odot^2 \Sigma v_*^2$.

Without a hydrodynamic simulation in 3-dimensions an accurate description is missing. Nevertheless it is sufficient to approximate the solution as that fraction of the disk matter that has an internal energy density, ϵ_{shk} greater than that of the ambient disk by that factor such that it will rise to a height, z , determined by its potential energy, or $\Delta\Phi = \frac{GMz^2}{2r^3}$ (equation (21)). Since $\Delta S/S_o = \epsilon_{shk}/\epsilon_o$, where $\epsilon_o \simeq \Delta\Phi(H) = \frac{GMH^2}{2r^3}$, then in order for a plume to rise above the disk mid-plane to a height, l ,

$$\left(\frac{l}{H}\right)^2 \simeq \left(\frac{\epsilon_{shk}}{\epsilon_o}\right) \simeq \left(\frac{v_K}{c_s}\right)^2 \left(\frac{R_\odot}{R_{shk}}\right)^2 \simeq \left(\frac{r}{H}\right)^2 \left(\frac{R_\odot}{R_{shk}}\right)^2. \quad (22)$$

We are concerned with plumes that rise well above the disk so that they can expand horizontally by a factor several times the plume's original radius. In this case the moment of inertia of the plume about its own axis will be increased by several times before falling back to the disk. This causes the plume to reduce its own rotation rate relative to the frame of the disk, that is to untwist relative to that frame. For this expansion to take place, the plume must rise roughly $\sim 2H$ above the disk, or $l \simeq 3H$. At this height the pressure of the hydrostatic isothermal atmosphere with the density profile as $\propto \exp(-z^2/H^2)$ becomes negligible compared to that of the plume, and so the hot gas of the plume can expand both vertically and horizontally as a free expansion. With this l we get

$$\frac{R_{shk}}{R_\odot} \simeq \frac{1}{3} \frac{r}{H}. \quad (23)$$

Using expression (8) for H/r at $r \leq r_{ab}$ we obtain

$$R_{shk} \simeq 0.24H \left(\frac{\alpha_{ss}}{0.01}\right)^{2/21} \left(\frac{l_E}{0.1}\right)^{-26/21} \left(\frac{\epsilon}{0.1}\right)^{26/21} M_8^{-19/21} \frac{r}{r_{ab}} \left(1 - \sqrt{\frac{3r_g}{r}}\right)^{-2}, \quad (24)$$

Thus a plume, starting from a size, $R_{shk} < H$ will expand to a size $\simeq 2H$ both vertically and horizontally, thus producing a near spherical bubble with radius $r_p = H$ above the disk. Post shock

expansion will increase the estimate of R_{shk} somewhat. For simplicity we will use $R_{shk} = H/2$ for estimates of the toroidal flux entrained in the plumes in paper II. This is our standard plume.

Finally we note that the rise and fall time of this plume should be the half orbit time, corresponding to a ballistic trajectory above and back to the surface of the disk. Hence, $t_{plume} \simeq \pi/\Omega$ or a plume rotation angle of π radians. We next consider the twisting of the plume leading to its effective helicity.

4.3. The Untwisting or Helicity Generation by the Plume

Thus the plume should expand to several times its original radius by the time it reaches the height of the order $2H$. The corresponding increase in the moment of inertia of the plume and the conservation of the angular momentum of the plume causes the plume to rotate slower relative to the inertial frame (Beckley et al. 2003; Mestel 1999; Colgate & Li 1999). From the viewpoint of the observer in the frame corotating with the Keplerian flow at the radius of the disk of the plume, this means that the plume rotates in the direction opposite to the Keplerian rotation with an angular velocity equal to some fraction of the local Keplerian angular velocity depending upon the radial expansion ratio. Since the expansion of the plume will not be infinite in the rise and fall time of π radians of Keplerian rotation of the disk, we expect that the average of the plume rotation will be correspondingly less, or $\Delta\phi < \pi$ or $\sim \pi/2$ radians. Any force or frictional drag that resists this rotation will be countered by the Coriolis force. Finally we note that kinetic helicity is proportional to

$$h = \mathbf{v} \cdot (\nabla \times \mathbf{v}). \quad (25)$$

For the dynamo one requires one additional dynamic property of the plumes. This is, that the total rotation angle must be finite and preferably $\simeq \pi/2$ radians, otherwise a larger angle or after many turns the vector of the entrained magnetic field would average to a small value and consequently the dynamo growth rate would be correspondingly small. This property of finite rotation, $\Delta\phi \sim \pi/2$ radians, is a fundamental property of plumes produced above a Keplerian disk.

5. Summary

Thus we have derived the approximate properties of an accretion disk around a massive black hole, the high probability of star-disk collisions, the three necessary properties of the resulting plumes all necessary for a robust dynamo. What is missing from this description is the necessary electrical properties of the medium. However, since the required conductivity is so closely related to the mechanism of the dynamo itself, we leave it to the following paper II (Pariev, Colgate & Finn 2006), a discussion of this remaining property of the hydrodynamic accretion disk flows necessary for a robust accretion disk dynamo. With this exception we feel confident that an accretion disk forming a CMBH with its associated star disk collisions is nearly ideal for forming a robust feed-

back-limited dynamo and thus, potentially converting a major fraction of the gravitational free energy of massive black hole formation into magnetic energy.

VP is pleased to thank Richard Lovelace and Eric Blackman for helpful discussions. Eric Blackman is thanked again for his support during the late stages of this work. SC particularly recognizes Hui Li of LANL for support through the Director funded Research on the Magnetized Universe and New Mexico Tech for support of the plume rotation experiments as well as the dynamo experiment. The facilities and interactions of Aspen Center for Physics during two summer visits by VP and more by SAC are gratefully acknowledged. This work has been supported by the U.S. Department of Energy through the LDRD program at Los Alamos National Laboratory. VP also acknowledges partial support by DOE grant DE-FG02-00ER54600 and by the Center for Magnetic Self-Organization in Laboratory and Astrophysical Plasmas at the University of Wisconsin-Madison.

A. Parameters of Shakura–Sunyaev Disk

In the subsequent estimates of the disk physical parameters we will keep the radius of the disk r , where the star-disk collisions happen, Shakura–Sunyaev viscosity parameter α_{ss} , ratio of the disk luminosity to the Eddington luminosity l_E , fraction ϵ of the rest mass accretion flux $\dot{M}c^2$, which is radiated away, as parameters. We will assume them to be within an order of magnitude from their typical values of importance for the dynamo problem, which are the following

$$\alpha_{ss} = 0.01, \quad l_E = 0.1, \quad \epsilon = 0.1, \quad r = 10^{-2} \text{ pc}. \quad (\text{A1})$$

The flux of the stars through the disk, $nv/4$, peaks at the radii inside $r = 10^{-2}$ pc (see section 3.2), therefore we need to know the physics of the accretion disk at $r \sim 10^{-2}$ pc. Below, we will define the gravitational radius as $r_g = 2GM/c^2 = 3.0 \cdot 10^{13} M_8 \text{ cm} = 9.5 \cdot 10^{-6} M_8 \text{ pc}$. All formulae for the structure of Shakura–Sunyaev disk are written for an arbitrary value of the black hole mass $M = 10^8 M_8 M_\odot$. However, we will consider only $M = 10^8 M_\odot$ whenever we invoke the model for the star distribution in the central cluster, because the best available model of the central star cluster was calculated for the $M = 10^8 M_\odot$ (section 2.1). Finally, the accuracy of expressions for the disk parameters is only one significant figure in all cases, and we keep two or even three figures only to avoid introducing additional round off errors, when using our expressions. Similarly, one should not be concerned about small jumps of values across the boundaries with different physical approximations: a more elaborate treatment is needed to find exact matching solutions there, although the physical principles are unchanged.

We use formulae from the Shakura & Sunyaev (1973) article to obtain estimate of the state of the accretion disk. We assume the Schwarzschild black hole with the inner edge of the disk being at $3r_g$. However, since we consider star-disk collisions happening at $\sim 10^3 r_g$, general relativistic corrections are only at a level less than few per cents and do not matter for our approximate

treatment of star-disk collision hydrodynamics. All expressions for disk quantities below were also verified in later textbooks by Shapiro & Teukolsky (1983) and Krolik (1999).

The inner part of the disk (part (a) as in Shakura & Sunyaev (1973)) is radiation dominated and the opacity is dominated by Thomson scattering. In the next zone (part (b)) the opacity is still Thomson, while the gas pressure exceeds radiation pressure. In the outer most zone (part (c)) the opacity becomes dominated by free-free and bound-free transitions. The boundary between parts (a) and (b) r_{ab} is given by an expression

$$r_{ab} = 236 r_g \left(\frac{\alpha_{ss}}{0.01} \right)^{2/21} \left(\frac{M}{10^8 M_\odot} \right)^{2/21} \left(\frac{l_E}{0.1} \right)^{16/21} \left(\frac{\epsilon}{0.1} \right)^{-16/21}. \quad (\text{A2})$$

The boundary between parts (b) and (c) r_{bc} is given by the following expression

$$r_{bc} = 3.4 \cdot 10^3 r_g \left(\frac{l_E}{0.1} \right)^{2/3} \left(\frac{\epsilon}{0.1} \right)^{-2/3}. \quad (\text{A3})$$

One can see that, generally, $r_{bc} > 10^{-2}$ pc. Therefore, we may consider zones (a) and (b) only, for our purpose of addressing star-disk collisions.

First, we will list parameters following from solving for the vertically averaged radial distributions of physical parameters inside the zone (a). The surface density is

$$\begin{aligned} \Sigma &= 407 \text{ g cm}^{-2} \frac{0.01}{\alpha_{ss}} \left(\frac{l_E}{0.1} \right)^{-1} \left(\frac{\epsilon}{0.1} \right) \left(\frac{rc^2}{GM} \right)^{3/2} \left(1 - \sqrt{\frac{3r_g}{r}} \right)^{-1} \\ &= 4.2 \cdot 10^6 \text{ g cm}^{-2} \left(\frac{\alpha_{ss}}{0.01} \right)^{-6/7} \left(\frac{l_E}{0.1} \frac{0.1}{\epsilon} \right)^{1/7} M_8^{1/7} \left(\frac{r}{r_{ab}} \right)^{3/2}. \end{aligned} \quad (\text{A4})$$

The half thickness of the disk is

$$H = 2.6 \cdot 10^{13} \text{ cm} \frac{l_E}{0.1} \left(\frac{\epsilon}{0.1} \right)^{-1} M_8 \left(1 - \sqrt{\frac{3r_g}{r}} \right). \quad (\text{A5})$$

This H depends upon the radius only via general relativistic corrections. So, the disk has asymptotically constant thickness for values of $r \gg r_g$ (Shakura & Sunyaev 1973; Krolik 1999). Moreover, H does not depend on α_{ss} in zone (a) and so H is also independent on the mechanism of angular momentum transport. The corresponding density is

$$\begin{aligned} \rho &= \frac{\Sigma}{2H} = 7.5 \cdot 10^{-7} \text{ g cm}^{-3} \frac{0.01}{\alpha_{ss}} \left(\frac{l_E}{0.1} \right)^{-2} \left(\frac{\epsilon}{0.1} \right)^2 \times \\ &\left(\frac{r}{10^{-2} \text{ pc}} \right)^{3/2} M_8^{-5/2} \left(1 - \sqrt{\frac{3r_g}{r}} \right)^{-2}. \end{aligned} \quad (\text{A6})$$

At the luminosity of an AGN

$$L = 1.3 \cdot 10^{45} \left(\frac{l_E}{0.1} \right) M_8 \text{ erg s}^{-1}, \quad (\text{A7})$$

the mass flux is

$$\dot{M} = 0.23 M_{\odot} \text{yr}^{-1} \left(\frac{0.1}{\epsilon} \right) \left(\frac{l_E}{0.1} \right) M_8 = 1.4 \cdot 10^{25} \text{ g s}^{-1} \left(\frac{0.1}{\epsilon} \right) \left(\frac{l_E}{0.1} \right) M_8. \quad (\text{A8})$$

The energy emitted from the unit surface of the one side of the disk per unit time is

$$Q = \frac{3}{8\pi} \dot{M} \frac{GM}{R^3} \left(1 - \sqrt{\frac{3r_g}{r}} \right) = 7.6 \cdot 10^8 \text{ erg cm}^{-2} \text{s}^{-1} \left(\frac{0.1}{\epsilon} \right) \left(\frac{l_E}{0.1} \right) \times \left(\frac{r}{10^{-2} \text{ pc}} \right)^{-3} M_8^2 \left(1 - \sqrt{\frac{3r_g}{r}} \right). \quad (\text{A9})$$

The effective temperature near the surface of the disk is

$$Q = \frac{ac}{4} T_s^4, \quad T_s = 1900 \text{ K} \left(\frac{0.1}{\epsilon} \right)^{1/4} \left(\frac{l_E}{0.1} \right)^{1/4} \times \left(\frac{r}{10^{-2} \text{ pc}} \right)^{-3/4} M_8^{1/2} \left(1 - \sqrt{\frac{3r_g}{r}} \right)^{1/4}. \quad (\text{A10})$$

The article by Shakura & Sunyaev (1973) contains the solution of the radiative transport equation in the vertical direction of an optically thick disk with assumed local thermodynamic equilibrium for each z in the disk. Volume emission due to viscous heating is included in the solution. Using this solution with the Thomson opacity $\kappa_T = 0.4 \text{ cm}^2 \text{g}^{-1}$ one obtains (section 2a of Shakura & Sunyaev 1973) the temperature at the midplane of the disk

$$T_{mpd}^4 = T_s^4 \left(1 + \frac{3}{16} \kappa_T \Sigma \right). \quad (\text{A11})$$

Since the disk is very opaque for Thomson scattering one can neglect 1 in the expression (A11) and obtains

$$T_{mpd} = T_s \cdot 41.3 \left(\frac{0.01}{\alpha_{ss}} \right)^{1/4} \left(\frac{l_E}{0.1} \right)^{-1/4} \left(\frac{\epsilon}{0.1} \right)^{1/4} \times \left(\frac{r}{10^{-2} \text{ pc}} \right)^{3/8} M_8^{-3/8} \left(1 - \sqrt{\frac{3r_g}{r}} \right)^{-1/4}. \quad (\text{A12})$$

Using expression (A10) for the effective surface temperature T_s and substituting for T_s in the equation (A12) one obtains

$$T_{mpd} = 7.9 \cdot 10^4 \text{ K} \left(\frac{0.01}{\alpha_{ss}} \right)^{1/4} \left(\frac{r}{10^{-2} \text{ pc}} \right)^{-3/8} M_8^{1/8}. \quad (\text{A13})$$

Note that the terms describing the dependence on the accretion rate cancel out as well as general relativistic correction term. Therefore, T_{mpd} in the inner parts of accretion disk does not depend on

the accretion rate, but is determined by the mass of the central black hole and viscosity parameter α_{ss} . Radiation pressure in the midplane of the disk in the zone (a) is

$$P_r = \frac{1}{3} a T_{mpd}^4 = 1.07 \cdot 10^5 \text{ erg cm}^{-3} \frac{0.01}{\alpha_{ss}} M_8^{1/2} \left(\frac{r}{10^{-2} \text{ pc}} \right)^{-3/2}. \quad (\text{A14})$$

By integrating surface density (A4) one can obtain the total mass of the disk inside radius r (assuming $r \gg r_g$)

$$M_{disk} = 10^8 M_\odot M_8 \left(\frac{r}{r_{sg}} \right)^{7/2}, \quad (\text{A15})$$

where the radius r_{sg} , inside of which the mass of the disk is equal to the mass of the black hole, is given by

$$r_{sg} = 1400 r_g \cdot M_8^{-2/7} \left(\frac{\alpha_{ss}}{0.01} \right)^{2/7} \left(\frac{l_E}{0.1} \right)^{2/7} \left(\frac{\epsilon}{0.1} \right)^{-2/7}. \quad (\text{A16})$$

Since the total mass of the disk grows very rapidly with the radius r , the gravitational potential of the disk would dominate the gravitational potential of the black hole for $r > r_{sg}$. As follows from comparing expressions (A2) and (A16) $r_{sg} > r_{ab}$ in general. More exactly, the condition $r_{sg} > r_{ab}$ reduces to

$$M_8^{-8/21} \left(\frac{\alpha_{ss}}{0.01} \right)^{4/21} \left(\frac{l_E}{0.1} \right)^{-10/21} \left(\frac{\epsilon}{0.1} \right)^{10/21} > 0.165. \quad (\text{A17})$$

The dependence of the left hand side of equation (A17) on the black hole mass M_8 and viscosity parameter α_{ss} is weak. One also expects the efficiency of radiation ϵ to be within the order of magnitude from the value 0.1. The largest variations are expected for the luminosity l_E . However, even for $l_E = 1$, still $r_{ab} < r_{sg}$. Generally, the mass of the inner zone of the disk is small compared to the mass of the black hole. Below we assume $r_{ab} < r_{sg}$ to be always satisfied. The total mass of the inner part of the disk enclosed inside $r < r_{ab}$ is

$$M(r_{ab}) = 1.83 \cdot 10^5 M_\odot \left(\frac{\alpha_{ss}}{0.01} \right)^{-2/3} M_8^{7/3} \left(\frac{l_E}{0.1} \right)^{5/3} \left(\frac{\epsilon}{0.1} \right)^{-5/3}, \quad (\text{A18})$$

which is, generally, much smaller than the mass $10^8 M_8 M_\odot$ of the black hole.

In the zone (b) the surface density is given by

$$\begin{aligned} \Sigma &= 1.75 \cdot 10^8 \text{ g cm}^{-2} \left(\frac{\alpha_{ss}}{0.01} \right)^{-4/5} \left(\frac{l_E}{0.1} \right)^{3/5} \left(\frac{\epsilon}{0.1} \right)^{-3/5} M_8^{1/5} \left(\frac{rc^2}{GM} \right)^{-3/5} \\ &= 4.4 \cdot 10^6 \text{ g cm}^{-2} \left(\frac{r}{r_{ab}} \right)^{-3/5} \left(\frac{\alpha_{ss}}{0.01} \right)^{-6/7} M_8^{1/7} \left(\frac{l_E}{0.1} \frac{0.1}{\epsilon} \right)^{1/7}. \end{aligned} \quad (\text{A19})$$

The integral of this surface density from r_{ab} to any given r gives the mass enclosed between r_{ab} and r as

$$\begin{aligned} M_b(r) &= 85 M_\odot \left[\left(\frac{r}{M} \right)^{7/5} - \left(\frac{r_{ab}}{M} \right)^{7/5} \right] \left(\frac{\alpha_{ss}}{0.01} \right)^{-4/5} \times \\ &\quad \left(\frac{l_E}{0.1} \right)^{3/5} \left(\frac{\epsilon}{0.1} \right)^{-3/5} M_8^{11/5}. \end{aligned} \quad (\text{A20})$$

Now we can estimate the value of $r = r_{sg}$ such that $M_b(r_{sg}) = 10^8 M_8 M_\odot$ (neglecting the contribution from the part (a) of the disk). Neglecting 1 compared to the ratio $r_{sg}/r_{ab} \gg 1$, one obtains

$$\frac{r_{sg}}{r_{ab}} \approx 46 M_8^{-20/21} \left(\frac{\alpha_{ss}}{0.01}\right)^{10/21} \left(\frac{l_E}{0.1}\right)^{-25/21} \left(\frac{\epsilon}{0.1}\right)^{25/21}. \quad (\text{A21})$$

The logarithmic width of the zone (b), i.e. the ratio r_{bc}/r_{ab} , is given by

$$\frac{r_{bc}}{r_{ab}} = 14.4 \left(\frac{\alpha_{ss}}{0.01}\right)^{-2/21} M_8^{-2/21} \left(\frac{l_E}{0.1}\right)^{-2/21} \left(\frac{\epsilon}{0.1}\right)^{2/21}, \quad (\text{A22})$$

i.e. almost a constant, depending on all parameters of the disk and the black hole very weakly. Depending upon parameters, r_{sg} maybe inside or outside the r_{bc} , however, as we show next, the disk in part (b) is unstable to fragmentation caused by self gravity, which makes the question on whether the exact position of r_{sg} is with respect to r_{bc} unimportant. The expressions for radiation flux Q and surface temperature of the disk T_s remain the same as in the part (a) of the disk, namely given by the expressions (A9) and (A10). For the temperature at the midplane of the disk one can obtain from formula (A11)

$$T_{mpd} = 3.5 \cdot 10^7 \text{ K} \left(\frac{\alpha_{ss}}{0.01}\right)^{-1/5} \left(\frac{0.1 l_E}{\epsilon 0.1}\right)^{2/5} \left(\frac{rc^2}{GM}\right)^{-9/10} M_8^{-1/5}. \quad (\text{A23})$$

The characteristic thickness of the disk is given by

$$H = 2.75 \cdot 10^{10} \text{ cm} \left(\frac{\alpha_{ss}}{0.01}\right)^{-1/10} \left(\frac{0.1 l_E}{\epsilon 0.1}\right)^{1/5} M_8^{9/10} \left(\frac{rc^2}{GM}\right)^{21/20}. \quad (\text{A24})$$

Then, from expressions (A19) and (A24), one can obtain the vertically averaged density in the zone (b) as

$$\rho = \frac{\Sigma}{2H} = 3.2 \cdot 10^{-3} \text{ g cm}^{-3} \left(\frac{\alpha_{ss}}{0.01}\right)^{-7/10} \left(\frac{l_E 0.1}{0.1 \epsilon}\right)^{2/5} M_8^{-7/10} \left(\frac{rc^2}{GM}\right)^{-33/20}. \quad (\text{A25})$$

The corresponding values of the radiation pressure $P_r = \frac{1}{3} a T_{mpd}^4$ and the gas pressure $P_g = 2nkT_{mpd}$ at the midplane are

$$P_r = 3.8 \cdot 10^{15} \text{ erg cm}^{-3} \left(\frac{\alpha_{ss}}{0.01}\right)^{-4/5} \left(\frac{0.1 l_E}{\epsilon 0.1}\right)^{8/5} \times \left(\frac{rc^2}{GM}\right)^{-18/5} M_8^{-4/5} \left(1 - \sqrt{\frac{3r_g}{r}}\right)^{8/5}, \quad (\text{A26})$$

$$P_g = 1.76 \cdot 10^{13} \text{ erg cm}^{-3} \left(\frac{\alpha_{ss}}{0.01}\right)^{-9/10} \left(\frac{0.1 l_E}{\epsilon 0.1}\right)^{4/5} \times \left(\frac{rc^2}{GM}\right)^{-51/20} M_8^{-9/10} \left(1 - \sqrt{\frac{3r_g}{r}}\right)^{4/5}. \quad (\text{A27})$$

Calculating the ratio of P_r to P_g one can recover the expression (A2) for the radius, when $P_r = P_g$.

When the disk becomes self gravitating, it may become subject to gravitational instability. Let us check that by calculating Toomre parameter $\text{To} = \frac{\varkappa c_s}{\pi G \Sigma}$ (e.g., Binney & Tremaine 1994). Epicyclic frequency \varkappa is equal to its value for the point mass M located at the position of the black hole $\varkappa = \Omega_K = (GM)^{1/2}/r^{3/2}$, since the mass of the disk is small compared to the mass of the black hole. Sound speed is equal to $c_s^2 = \frac{kT_{mpd}}{m_p}$ in zone (b) and $c_s^2 = \frac{P_r}{\rho}$ in the zone (a) (a coefficient close to 1 is neglected). Substituting appropriate expressions we obtain for the sound speed in zone (b)

$$c_s = 5.37 \cdot 10^7 \text{ cm s}^{-1} \left(\frac{\alpha_{ss}}{0.01} \right)^{-1/10} \left(\frac{0.1 l_E}{\epsilon \cdot 0.1} \right)^{1/5} \times \left(\frac{rc^2}{GM} \right)^{-9/20} M_8^{-1/10} \left(1 - \sqrt{\frac{3r_g}{r}} \right)^{1/5}, \quad (\text{A28})$$

in zone (a)

$$c_s = 3.5 \cdot 10^{10} \text{ cm s}^{-1} \frac{l_E}{0.1} \left(\frac{\epsilon}{0.1} \right)^{-1} \left(\frac{rc^2}{GM} \right)^{-3/2} \left(1 - \sqrt{\frac{3r_g}{r}} \right). \quad (\text{A29})$$

The Toomre parameter becomes in zone (a)

$$\begin{aligned} \text{To} &= 8.33 \cdot 10^{11} \frac{\alpha_{ss}}{0.01} \left(\frac{l_E}{0.1} \right)^2 \left(\frac{\epsilon}{0.1} \right)^{-2} \left(\frac{rc^2}{GM} \right)^{-9/2} M_8^{-1} \left(1 - \sqrt{\frac{3r_g}{r}} \right)^2 \\ &= 0.77 \left(\frac{\alpha_{ss}}{0.01} \right)^{4/7} M_8^{-10/7} \left(\frac{l_E}{0.1} \right)^{-10/7} \left(\frac{\epsilon}{0.1} \right)^{10/7} \left(\frac{r}{r_{ab}} \right)^{-9/2} \end{aligned} \quad (\text{A30})$$

and in the zone (b)

$$\begin{aligned} \text{To} &= 2.97 \cdot 10^3 \left(\frac{\alpha_{ss}}{0.01} \right)^{7/10} \left(\frac{0.1 l_E}{\epsilon \cdot 0.1} \right)^{-2/5} M_8^{-13/10} \left(\frac{rc^2}{GM} \right)^{-27/20} \\ &= 0.73 \left(\frac{r}{r_{ab}} \right)^{-27/20} M_8^{-10/7} \left(\frac{\alpha_{ss}}{0.01} \right)^{4/7} \left(\frac{l_E \cdot 0.1}{0.1 \cdot \epsilon} \right)^{-10/7} \\ &= 9.7 \cdot 10^{-2} \left(\frac{\alpha_{ss}}{0.01} \right)^{7/10} \left(\frac{l_E \cdot 0.1}{0.1 \cdot \epsilon} \right)^{-2/5} M_8^{1/20} \left(\frac{r}{0.01 \text{ pc}} \right)^{-27/20}. \end{aligned} \quad (\text{A31})$$

Gravitational instability develops if $\text{To} < 1$. One can see from expressions (A30) and (A31) that To strongly declines with increasing the radius. The disk has a well defined outer radius of gravitational stability r_T such that $\text{To}(r_T) = 1$. For our fiducial parameters, r_T is close to the r_{ab} . At the outer edge of the zone (b) one has

$$\text{To}(r_{bc}) = 2.0 \cdot 10^{-2} \left(\frac{\alpha_{ss}}{0.01} \right)^{7/10} M_8^{-13/10} \left(\frac{l_E \cdot 0.1}{0.1 \cdot \epsilon} \right)^{-13/10}. \quad (\text{A32})$$

Large values of α_{ss} , small masses of the central black hole, and low accretion rates cause the To to increase and can cause the radius r_T to become larger than r_{ab} . As follows from expression (A30) the value for r_T (when $r_T < r_{ab}$) is

$$\begin{aligned} r_T &\approx r_{ab} \left(\frac{\alpha_{ss}}{0.01}\right)^{8/63} M_8^{-20/63} \left(\frac{l_E}{0.1}\right)^{-20/63} \left(\frac{\epsilon}{0.1}\right)^{20/63} \left(1 - \sqrt{\frac{3r_g}{r}}\right)^{4/9} \\ &= 218r_g M_8^{-2/9} \left(\frac{\alpha_{ss}}{0.01}\right)^{2/9} \left(\frac{0.1 l_E}{\epsilon 0.1}\right)^{4/9}. \end{aligned} \quad (\text{A33})$$

Assuming the range of parameters $1 > \alpha_{ss} > 10^{-3}$, $10^{-2} < M_8 < 10^2$, $10^{-3} < l_E < 1$, and $\epsilon \approx 0.1$ the lowest possible location of r_T will be at $\approx 6r_g$, i.e. in the vicinity of the inner edge of the disk, where the Toomre stability criterion is not directly applicable. On the other side, the stable region of the disk can extend over the whole of zone (b) and into the outermost zone (c) as well. At the radius of $r = 0.01$ pc and $M_8 = 1$, which corresponds to the width of the broad line region, the disk would be unstable for the fiducial set of parameters. However, at lower values of accretion rates $l_E \leq 0.01$, which are expected in the case of relatively low activity in Seyfert galaxies, and larger values of $\alpha_{ss} \geq 0.1$ the stable part of the disk will include 0.01 pc.

REFERENCES

- Armitage, P.J., Zurek, W.H., & Davies, M.B. 1996, ApJ, 470, 237
- Artemova, I.V., Bisnovatyi–Kogan, G.S., Björnsson, G., & Novikov, I.D. 1996, ApJ, 456, 119
- Artymowicz, P., Lin, D.N.C., & Wampler, E.J. 1993, ApJ, 409, 592
- Artymowicz, P. 1994, ApJ, 423, 581
- Bahcall, J.N., & Wolf, R.A. 1976, ApJ, 209, 214
- Balbus, S.A., & Hawley, J.F. 1998, Rev. of Modern Physics, 70, 1
- Beckley, H.F., Colgate, S.A., Romero, V.D., & Ferrel, R. 2003, ApJ, 599, 702
- Binney, J., & Tremaine, S. 1994, Galactic Dynamics. (Princeton: Princeton University Press)
- Biskamp, D. 1993, Nonlinear Magnetohydrodynamics. (Cambridge: Cambridge Univ. Press)
- Bisnovatyi-Kogan, G.S. 2002, Stellar Physics. 2: Stellar Evolution and Stability. (Berlin: Springer–Verlag)
- Blandford, R.D. 1976, MNRAS, 176, 465
- Bourgoin, L., Odier, P., Pinton, J.-F., & Ricard, Y. 2004, Phys. Fluids, 16, 2529.

- Brandenburg, A., & Schmitt, D. 1998, *A&A*, 338, L55
- Bromley, B.C., Miller, W.A., & Pariev, V.I. 1998, *Nature*, 391, 54
- Busse, F.H. 1991, in *Advances in Solar System Magnetohydrodynamics*, eds. Priest E.R., Wood A.W. (Cambridge: Cambridge Univ. Press), p. 51
- Chakrabarti, S.K., Rosner, R., & Vainshtein, S.I. 1994, *Nature*, 368, 434
- Childress, S., Collet, P., Frish, U., Gilbert, A.D., Moffatt, H.K., & Zaslavsky, G.M. 1990, *Geophys. Astrophys. Fluid Dyn.*, 52, 263.
- Colgate, S.A., & Li, H. 1997, in *Relativistic Jets in AGNs*, ed. Ostrowski M. (Crakow: Poland), p. 170
- Colgate, S.A., & Li, H. 1999, *Ap&SS*, 264, 357
- Colgate, S.A., Li, H., & Pariev, V.I. 2001, *Physics of Plasmas*, 8, 2425
- Colgate, S.A., Cen, R., Li, H., Currier, N., & Warren, M.S. 2003, *ApJ*, 598, L7
- Courant, R., & Friedrichs, K.O. 1948, *Supersonic Flow and Shock Waves*. (New York: Interscience Pub.)
- Cowling, T.G. 1981, *ARA&A*, 19, 115
- Drake, J.F., Swisdak, M., Cattell, C., Shay, M.A., Rogers, B.N., & Zeiler, A. 2003, *Science*, 299, 873
- Fabian, A.C., Nandra, K., Reynolds, C.S., Brandt, W.N., Otani, C., Tanaka, Y., Inoue, H., & Iwasawa, K. 1995, *MNRAS*, 277, L11
- Fabian A.C., Iwasawa K., Reynolds C.S., Young A.Y. 2000, *PASP*, 112, 1145
- Field, G.B., Blackman, E.G., Chou, H. 1999, *ApJ*, 513, 638
- Gailitis, A., Lielausis, O., Dement'ev, S., et al. 2000, *Phys. Rev. Lett.*, 84, 4365
- Gailitis, A., Lielausis, O., Platacis, E., et al. 2001, *Phys. Rev. Lett.*, 86, 3024
- Goodman, J. 2003, *MNRAS*, 339, 937.
- Hubeny, I., & Hubeny, V. 1997, *ApJ*, 484, 37
- Hubeny, I., & Hubeny, V. 1998, *ApJ*, 505, 558
- Kormendy, J., Bender, R., Evans, A.S., & Richstone, D. 1998, *AJ*, 115, 1823
- Krause, F., & Rädler, K.H. 1980, *Mean-Field Magnetohydrodynamics and Dynamo Theory*. (Oxford: Pergamon Press)

- Krolik, J.H. 1999, *Active Galactic Nuclei: From the Central Black Hole to the Galactic Environment*. (Princeton: Princeton University Press)
- Kronberg, P.P. 1994, *Rep. Prog. Phys.*, 57, 325
- Kronberg, P.P., Dufton, Q.W., Li, H., & Colgate, S.A. 2001, *ApJ*, 560, 178
- Landry, S., & Pineault, S. 1998, *MNRAS*, 296, 359
- Lauer, T.R., Ajhar, E.A., Byun, Y.-I., Dressler, A., Faber, S.M., Grillmair, C., Kormendy, J., Richstone, D., & Tremaine, S. 1995, *AJ*, 110, 2622
- Li, H., Finn, J.M., Lovelace, R.V.E., & Colgate, S.A. 2000, *ApJ*, 533, 1023
- Li, H., Lovelace, R.V.E., Finn, J.M., & Colgate, S.A. 2001a, *ApJ*, 561, 915
- Li, H., Colgate, S.A., Wendroff, B., & Liska, R. 2001b, *ApJ*, 551, 874
- Li, H., Nishimura, K., Barnes, D.C., Gary, S.P., & Colgate, S.A. 2003, *Physics of Plasmas*, 10, 2763
- Lovelace, R.V.E. 1976, *Nature*, 262, 649
- Lovelace, R.V.E., Li, H., Colgate, S.A., & Nelson, A.F. 1999, *ApJ*, 513, 805
- Lovelace, R.V.E., Li, H., Koldoba, A.V., Ustyugova, G.V., & Romanova, M.M. 2002, *ApJ*, 572, 445
- Lynden-Bell, D. 1996, *MNRAS*, 279, 389
- Merritt, D., & Ferrarese, L. 2001, *ApJ*, 547, 140
- Mestel, L. 1999, *Stellar Magnetism*. (Oxford: Clarendon)
- Moffatt, H.K. 1978, *Magnetic Field Generation in Electrically Conducting Fluids*. (Cambridge: Cambridge University Press)
- Moss, D., Shukurov, A., & Sokoloff, D. 1999, *A&A*, 343, 120
- Novikov, I.D., & Thorne, K.S. 1973, in *Black Holes*, eds. DeWitt C., DeWitt B.S. (New York: Gordon and Breach), p. 343
- Owen, F.N., Hardee, P.E., & Bignell, R.C. 1980, *ApJ*, 239, L11
- Pariev, V.I., Colgate, S.A., & Finn, J.M. 2006, *ApJ*, in press (paper II)
- Parker, E.N. 1955, *ApJ*, 121, 29
- Parker, E.N. 1979, *Cosmical Magnetic Fields, their Origin and their Activity*. (Oxford: Clarendon)
- Parker, E. 1992, *ApJ*, 401, 137

- Priest, E.R. 1982, *Solar Magneto-hydrodynamics*. (Boston: Kluwer, Inc.)
- Quinlan, G.D., & Shapiro, S.L. 1990, *ApJ*, 356, 483
- Rauch, K.P. 1995, *MNRAS*, 275, 628
- Rauch, K.P. 1999, *ApJ*, 514, 725
- Rephaeli, Y., & Salpeter, E.E. 1980, *ApJ*, 240, 20
- Roberts, P.H., & Soward, A.M. 1992, *Ann. Rev. of Fluid Mechanics*, 24, 459
- Schmitt, D. 1987, *A&A*, 174, 281
- Sedov, L.I. 1959, *Similarity and Dimensional Methods in Mechanics*. (New York: Academic Press)
- Shakura, N.I. 1972, *AZh*, 49, 921
- Shakura, N.I., & Sunyaev, R.A. 1973, *A&A*, 24, 337
- Shapiro, S.L., & Teukolsky, S.A. 1983, *Black Holes, White Dwarfs, and Neutron Stars*. (New York: Wiley-Interscience)
- Shlosman, I., & Begelman, M.C. 1989, *ApJ*, 341, 685
- Spence, E.J., Nornberg, M.D., Jacobson, C.M., Kendrick, R.D., & Forest, C.B. 2006, *Phys. Rev. Lett.*, 96, 055002.
- Steenbeck, M., Krause, F., & Rädler, K.H. 1966, *Z. Naturforsch.*, 21a, 369
- Steenbeck, M., & Krause, F. 1969a, *Astron. Nachr.*, 291, 49
- Steenbeck, M., & Krause, F. 1969b, *Astron. Nachr.*, 291, 271
- Stieglitz, R., & Müller, U. 2001, *Physics of Fluids*, 13, 561
- Stix, M. 1975, *A&A*, 42, 85
- Sulentic, J.W., Marziani, P., & Dultzin-Hacyan, D. 2000, *ARA&A*, 38, 521
- Syer, D., Clarke, C.J., & Rees, M.J. 1991, *MNRAS*, 250, 505
- Tanaka, Y., Nandra, K., Fabian, A.C., Inoue, H., Otani, C., Dotani, T., Hayashida, K., Iwasawa, K., et al. 1995, *Nature*, 375, 659
- Tremaine, S., Gebhardt, K., Bender, R., et al. 2002, *ApJ*, 574, 740
- Ustyugova, G.V., Lovelace, R.V.E., Romanova, M.M., Li, H., & Colgate, S.A. 2000, *ApJ*, 541, L21
- Vainshtein, S.I., & Cattaneo, F. 1992, *ApJ*, 393, 165

- Vainshtein, S.I., Parker, E.N., & Rosner, R. 1993, *ApJ*, 404, 773
- van der Marel, R.P. 1999, *AJ*, 117, 744
- van der Marel, R.P., de Zeeuw, P., Rix, H.-W., & Quinlan, G.D. 1997, *Nature*, 385, 610
- Vokrouhlicky, D., & Karas, V. 1998, *MNRAS*, 293, 1
- Wandel, A., & Petrosian, V. 1988, *ApJ*, 329, L11
- Zeldovich, Ya.B., & Raizer, Yu.P. 1967, *Physics of Shock Waves and High Temperature Hydrodynamic Phenomena*. (London: Academic Press)
- Zeldovich, Ya.B., Ruzmaikin, A.A., & Sokoloff, D.D. 1983, *Magnetic Fields in Astrophysics*. (New York: Gordon and Breach Science Publishers)
- Zurek, W.H., Siemiginowska, A., & Colgate, S.A. 1994, *ApJ*, 434, 46
- Zurek, W.H., Siemiginowska, A., & Colgate, S.A. 1996, *ApJ*, 470, 652

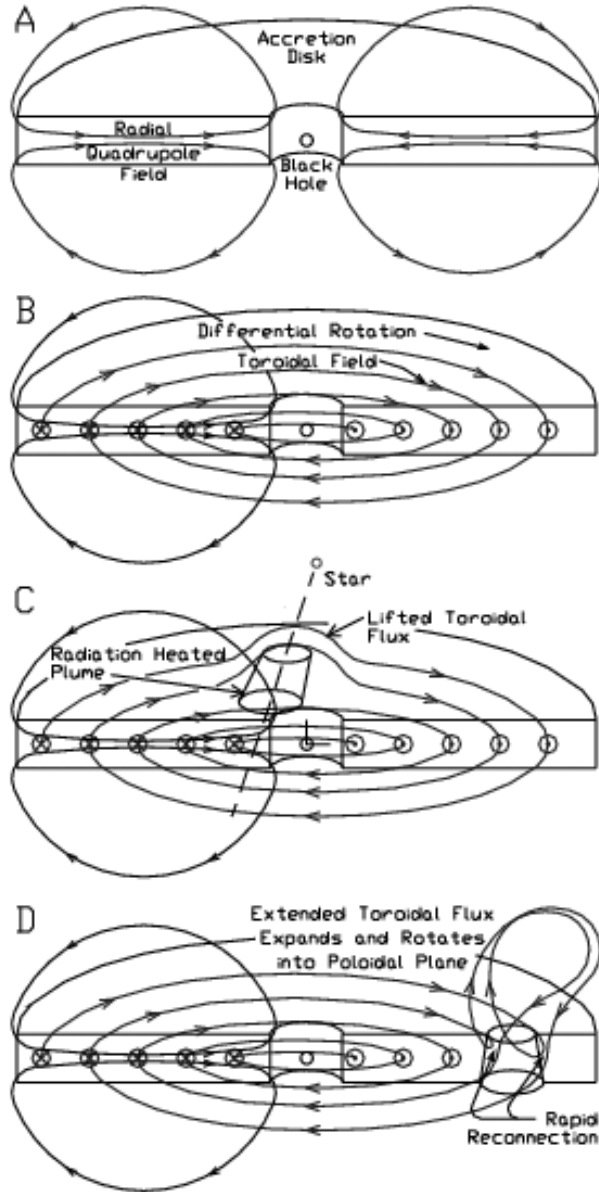


Fig. 1.— The $\alpha - \Omega$ dynamo in a galactic black hole accretion disk. The radial component of the poloidal quadrupole field within the disk (A) is sheared by the differential rotation within the disk, developing a stronger toroidal component (B). As a star passes through the disk it heats by shock and by radiation a fraction of the matter of the disk, which expands vertically and lifts a fraction of the toroidal flux within an expanding plume (C). Due to the conservation of angular momentum, the expanding plume and embedded flux rotate $\sim \pi/2$ radians before the matter in the plume and embedded flux falls back to the disk (D). Reconnection allows the new poloidal flux to merge with and augment the original poloidal flux (D).